The Very Deep Origin of the World's Biggest Diamonds

Evan M. Smith, Steven B. Shirey, and Wuyi Wang

Large and relatively pure diamonds like the historic 3,106 ct Cullinan, found in South Africa in 1905, have long been regarded as unusual based on their physical characteristics. For example, they often exhibit exceptional color and clarity, while routinely qualifying as type IIa, a rare designation of chemical purity. A new research discovery about these Cullinan-like diamonds is that they contain heretofore unknown, deeply derived inclusions that originate below the continental mantle keel and are thus known as "superdeep" diamonds (Smith et al., 2016). Originating from a depth between 360 and 750 km, they reveal information about the conditions within the convecting mantle, beneath the earth's rigid tectonic plates. Here we review the previously published findings, compare the Cullinan-like diamonds to the more abundant lithospheric diamond population, and offer evidence from some additional diamond samples that further verifies their superdeep origin. Cullinan-like diamonds contain minute and rare silicate and iron-rich metallic inclusions surrounded by a fluid jacket composed of methane and hydrogen. The inclusion compositions suggest that this deep mantle environment contains small pockets of oxygen-deficient metallic liquid out of which the diamonds crystallized. This new and unexpected observation made on the world's most expensive diamonds is important for understanding the chemical reactions between mineral assemblages in the deep earth. It shows that deep regions of the mantle contain metallic iron, as opposed to the shallower, more oxidized mantle rocks actively participating in plate tectonics and its associated volcanism.

Diamonds, besides being the most valuable gemstones for jewelry, are some of the most scientifically valuable samples of the deep earth. Interpretation of their included minerals and crystallization history provides a snapshot of otherwise inaccessible geological processes from more than 100 kilometers underground and often from billions of years in the past (e.g., Shirey and Shigley, 2013). No other mineral sample can provide information for research from such depths and from so long ago. Until recently, exceptional gem diamonds such as the famous Cullinan or Lesotho Promise, with a set of physical characteristics that distinguish them from other kinds of diamonds, were enigmatic and had an unknown origin (Bowen et al., 2009; Gurney and Helmstaedt, 2012; Moore, 2014). How did they form? Certainly not like 99% of other gem diamonds. New research carried out in the last two years at GIA, the Carnegie Institution for Science, and the University of Padua reveals that these Cullinan-like diamonds form in a geologically special way, involving metallic liquid and originating from extreme depths in Earth's mantle well below that of other gem diamonds (Smith et al., 2016).

RECOGNITION OF A NEW DIAMOND VARIETY

As a family, these diamonds tend to be large, inclusion-poor, and relatively pure (usually type IIa), and in their rough state they are irregularly shaped and significantly resorbed (figure 1) (Bowen et al., 2009; Gurney and Helmstaedt, 2012; Moore, 2014; Smith et al., 2016). These characteristics are combined in the acronym "CLIPPIR" (Cullinan-like, Large, Inclusion-Poor, Pure, Irregular, and Resorbed). Figure 2 shows a broad dataset of assorted diamonds, where the CLIPPIR population displays these characteristics. Among larger diamonds, there is a striking increase in the prevalence of D color grades and the proportion of type IIa diamonds, chiefly due to their

See end of article for About the Authors and Acknowledgments.
Gems & Gemology, Vol. 53, No. 4, pp. 388–403,
http://dx.doi.org/10.5741/GEMS.53.4.388

Figure 1. Rough CLIPPIR diamonds have physical features akin to the historic Cullinan diamond, which forms the "C" of the CLIPPIR acronym. The size distribution for this variety of diamond is skewed toward large sizes, with the examples shown here ranging from 14 to 91 carats. In rough form, CLIPPIR diamonds are irregularly shaped rather than well-formed crystals and sometimes appear to be broken fragments of once larger diamonds. Photo by Robert Weldon/GIA; courtesy of Gem Diamonds Ltd.

lack of nitrogen. As expected, these larger type IIa diamonds have very few inclusions and consequently high clarity grades.

Historically, it has been difficult to study these diamonds because of their rarity and high value as gemstones; they simply cannot be purchased for in-depth analysis on a research budget. It is only through the research program of GIA, where thousands of high-quality gem diamonds were available to be examined by non-destructive methods such as Raman spectroscopy and X-ray diffraction, that their common inclusion paragenesis and hence their origin was revealed. Here we review in more detail the key features of diamonds reported by Smith et al. (2016) as well as some additional CLIPPIR samples examined since.

An important key to the origin of these diamonds lies in the special inclusions they contain, composed of iron-nickel metal with minor sulfur and carbon. At the ambient pressure and temperature under which the CLIPPIR diamonds formed, these inclusions were metallic liquids. But now, under surface conditions, they have cooled and crystallized to a distinctive, rarely seen mineral assemblage. This assemblage includes the rare mineral cohenite, an iron-rich carbide with the formula $(Fe,Ni)_3C$, and the relatively common iron sulfide mineral pyrrhotite.

Metallic iron-nickel alloy is thought to be created and stabilized in parts of the deep mantle (Frost et al., 2004; Rohrbach et al., 2007). Although the normal amount of metal in these regions of the mantle is likely about 1% or less, it is expected to regulate and limit the local activity of oxygen (Frost et al., 2004). Oxygen availability is a key planetary parameter resulting from the earth's large-scale geologic evolution (Rohrbach and Schmidt, 2011). It controls, along with temperature and pressure, the basic mineral composition of the planet's interior, how this varies with depth, and the composition of melts generated. At the pressure and temperature conditions near and at Earth's surface, rocks almost never contain metallic iron. Also, these shallower rocks are affected by magmatism associated with plate tectonics and by interaction with Earth's atmosphere and hydrosphere,

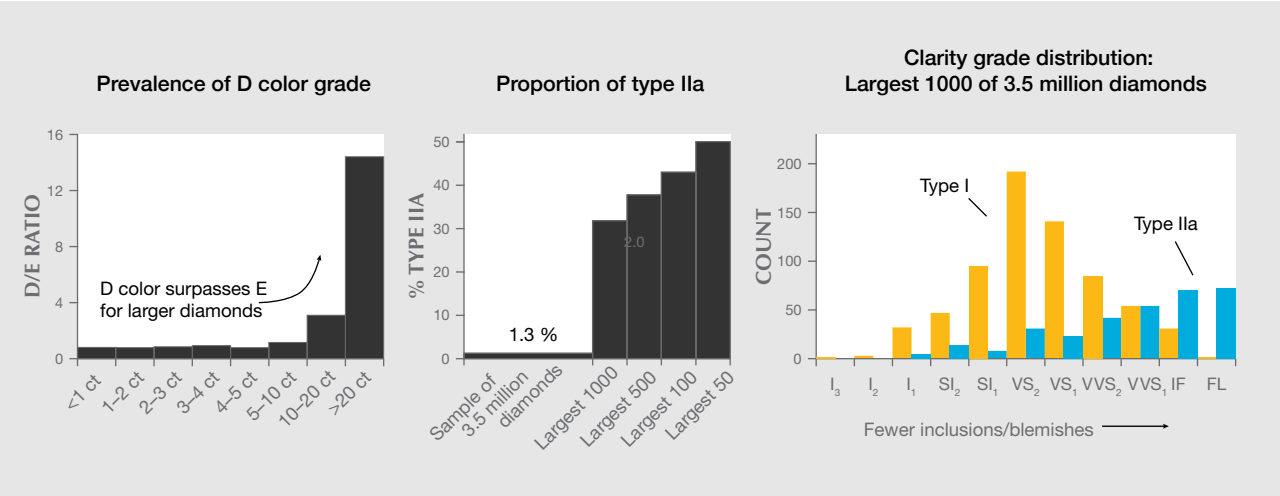

Figure 2. Systematic deviations of properties suggest that CLIPPIR diamonds become more prevalent among larger-sized diamonds. Left: Diamonds over 5 carats show an increasing incidence of D color grades in a random sample of 4.2 million diamonds graded by GIA; shown is the ratio of D color (colorless) to E color (not quite perfectly colorless) grades awarded. Center: In a similar dataset of 3.5 million samples, the proportion of type IIa diamonds (nitrogen-deficient, high-purity) also increases dramatically when considering only the larger diamonds. Right: Among a set of large diamonds, all over 15 carats, those qualifying as type IIa have markedly higher clarity and dominate the flawless grade category. (GIA clarity abbreviations: FL = flawless, IF = internally flawless, $VVS_{1/2}$ = very very slightly included 1/2, $VS_{1/2}$ = very slightly included 1/2, $SI_{1/2}$ = slightly included 1/2, and $I_{1/2/3}$ = included 1/2/3)

which occur at relatively oxidizing conditions. These conditions completely mask the ambient conditions in the earth's deep interior, which can be revealed in the mineralogy of CLIPPIR inclusions. It is coincidental but agreeably fitting that the world's most valuable diamonds as gemstones have now taken on exceptional scientific value.

NITROGEN AND THE DISTINCTION BETWEEN TYPE IIA AND CLIPPIR DIAMONDS

Nitrogen is all around us every day, making up 78% of the air we breathe and forming an essential element for life on Earth. Nitrogen behavior inside the earth, especially in minerals and fluids deep in the mantle, is less understood, but nitrogen is thought to be recycled into the mantle by plate tectonic activity. In the mantle, it is an ingredient in the diamond-forming fluids for the most common diamonds, known as type I. As such it is the most abundant trace element in diamond, where it substitutes for carbon atoms in the crystal structure. Since the advent of studies to understand the geological conditions for diamond growth and formation, diamonds have become one of the important tools that can help geologists trace the deep cycling and behavior of nitrogen.

The nitrogen content of diamond can vary greatly for several reasons, including variable supply of nitrogen in diamond-forming fluids, variable partitioning into the diamond, and variable partitioning into a competing nitrogen-bearing phase. Diamonds with no appreciable nitrogen-related absorption in the 800–1400 cm^{-1} range in infrared spectroscopy are classically defined as type IIa (Wilks and Wilks, 1994). Note that the abundance of nitrogen in diamond is a continuous range without a sharp division. The continuous range means that the 5–20 ppm nitrogen concentration threshold that marks the boundary in classification between type IIa (nitrogen-deficient) and type I (nitrogen-bearing) has no basis in mineralogy but rather is based on analytical sensitivity. Analytical sensitivity has shifted to lower thresholds over time, as instrumentation has improved.

The type IIa designation of chemical purity is usually regarded as a desirable gemological trait that is associated with high clarity and color, and it has proven convenient for scientific classification of diamond (see review by Breeding and Shigley, 2009). With one exception, the CLIPPIR diamonds of this study are type IIa. The relationship between CLIPPIR and type IIa diamonds likely applies to larger unstudied populations, as shown by the disproportionate

number of large, high-quality diamonds that are type IIa (figure 2). It is important to bear in mind, however, that not all type IIa diamonds are classified as CLIPPIR, and vice versa. Some lithospheric diamonds from peridotitic and eclogitic host rocks, for example, can also have very low nitrogen concentrations and be considered type IIa (e.g., Stachel and Harris, 2009; Gurney et al., 2010; Moore, 2014).

SOLIDIFIED IRON-NICKEL METAL: A NEWLY RECOGNIZED INCLUSION TYPE

Although inclusions are scarce in CLIPPIR diamonds, with the right approach they can be sought and studied. By leveraging a high-volume diamond grading service like that of GIA to find prospective samples for examination, it was possible to cull out enough of the rare inclusion-bearing CLIPPIR diamonds to look at their features as a group. In the past, the only reported inclusions in CLIPPIR diamonds were flat black inclusions with round boundaries, previously assumed to be flecks of graphite (Bowen et al., 2009; Moore, 2014). Rarely, some inclusions have been suspected to be sulfides, as they can resemble common pyrrhotite and pentlandite inclusions in lithospheric diamonds (Bowen, pers. comm., 2013, in Moore, 2014). However, a search of the literature reveals that the only consistently reported inclusion is visually identified graphite. In fact, the Cullinan diamond itself was described as having a small round, black inclusion in the center, which was intentionally bisected with the first cleave of the rough diamond by Joseph Asscher in 1908 (Crookes, 1909). Of course, the finished Cullinan gemstones are essentially flawless and free of inclusions (Scarratt and Shor, 2006). What few inclusions are to be found in rough CLIPPIR diamonds are usually eliminated during cutting and polishing, making the search for inclusions all the more difficult among polished goods.

In Brief

- Unusually large and pure diamonds like the 3,106 ct Cullinan have a special geological origin, much deeper in the earth's mantle than most other gem diamonds.
- Many of the world's biggest high-clarity, D-color diamonds belong to this special variety known as CLIPPIR diamonds.
- Newly recognized iron-rich metallic inclusions in these diamonds provide insight into the makeup of the deep earth.
- There is still much to be learned from the study of diamonds, which are an invaluable "window" into the unseen world deep beneath our feet.

Our recent study (Smith et al., 2016), comprising a targeted subset from hundreds of thousands of faceted diamonds as well as a small number of offcuts trimmed from rough diamonds during cutting and faceting, documented 53 inclusion-bearing CLIPPIR diamonds that establish a specific inclusion assemblage that deviates from known lithospheric or sublithospheric suites. Thirty additional faceted stones have since been studied and now yield observations on a total of 83 diamonds, summarized in table 1 (see also data supplement at www.gia.edu/gems-gemology/winter-2017-worlds-biggest-diamonds; for methods, see Smith et al., 2016). Past visual descriptions of inclusions in these types of diamonds mention flat, black features, interpreted as graphite. Our work has shown that these are graphitic rosette fractures that surround and sometimes conceal a much smaller non-graphitic inclusion (figure 3) somewhat reminiscent of sulfide inclusions.

In the center of the black fractures, the inclusion nucleus itself is different from that of a typical sulfide inclusion. In contrast to lithospheric diamonds, where black fracture rosettes are typically associated with sulfide inclusions, CLIPPIR diamonds have black fractures surrounding many inclusions, such that even silicates can have a superficial resemblance to "common" sulfide inclusions (figure 4A; see also figures S2 and S3 in Smith et al., 2016). The fractures are likely due to the higher stresses that build up around most superdeep inclusions when they are exhumed from the mantle.

The most common inclusion identified in CLIPPIR diamonds is a metallic iron-nickel-carbon-sulfur mixture. While most of these inclusions can only be studied remotely through the diamond by Raman spectroscopy, all inclusions that can be examined directly by other microanalytical techniques such as scanning electron microscopy (SEM), electron microprobe analysis, and/or X-ray diffraction (XRD) are similar metallic Fe-Ni-C-S mixtures. In our experience, these metallic inclusions differ from sulfide inclusions, which also have metallic luster but are smoother, more equant cuboctahedral shapes, isolated rather than grouped, and far less magnetic. The sulfide inclusions sometimes have brassy colors and identifiable sulfide mineral Raman features, and they have not yet been found to have coexisting fluid. In contrast, the Fe-Ni-

C-S metallic inclusions often have step-faced surfaces, strong magnetism, and elongate and irregular shapes, grouping into chains, and routinely possess a coexisting fluid phase (again, see figure 3).

Specifically, these inclusions are accompanied by a thin, invisible fluid layer of methane (CH_4) and lesser hydrogen (H_2) trapped at the interface between the solid inclusion and surrounding diamond (figure 5). Detailed analysis of the inclusions reveals that they are made up of cohenite ($(Fe, Ni)_3C$), interstitial Fe-Ni alloy, segregations of Fe-sulfide, and minor occasional Fe-Cr oxide, Fe-oxide (likely wüstite), and Fe-phosphate (Smith et al., 2016). We interpret the minor oxides as evidence of small amounts of oxygen even in these relatively oxygen-poor conditions, because all the inclusions examined were carefully selected from unaltered diamonds that had no surface-reaching fractures. This assemblage of minerals is interpreted to have crystallized during transport to the surface from the molten metallic liquid that was trapped during diamond growth at depth. The metal contains very limited amounts of oxygen, which indicates that CLIPPIR diamonds form under reducing conditions in the mantle. Metallic Fe-Ni-C-S melt inclusions such as these have not been described previously, although rare, isolated occurrences of native iron, iron-nickel alloy, and iron carbide inclusions have been found in other diamonds (Sharp, 1966; Jacob et al., 2004; Kaminsky and Wirth, 2011; Mikhail et al., 2014). Coincidentally, the German mineralogist Emil Cohen, for whom cohenite is named, might have encountered one of these Fe-Ni-C-S melt inclusions in an 80 ct rough diamond in South Africa 140 years ago, though he described the inclusion as "specular iron" or hematite based on color, luster, and form ("Iron in diamonds," 1877).

Figure 3. Examples of the typical appearance of metallic Fe-Ni-C-S inclusions in CLIPPIR diamonds. A: Two parallel <111> oriented chains (field of view 2.34 mm). B: Backlit inclusion chain (field of view 1.42 mm). C: Elongate metallic inclusion with a round black fracture of {111} orientation that obliquely cuts the <111> elongation direction of the inclusion (field of view 1.42 mm). D: A less elongate metallic inclusion with a small irregular tail on the lower left (field of view 1.42 mm). Photos by Evan M. Smith.

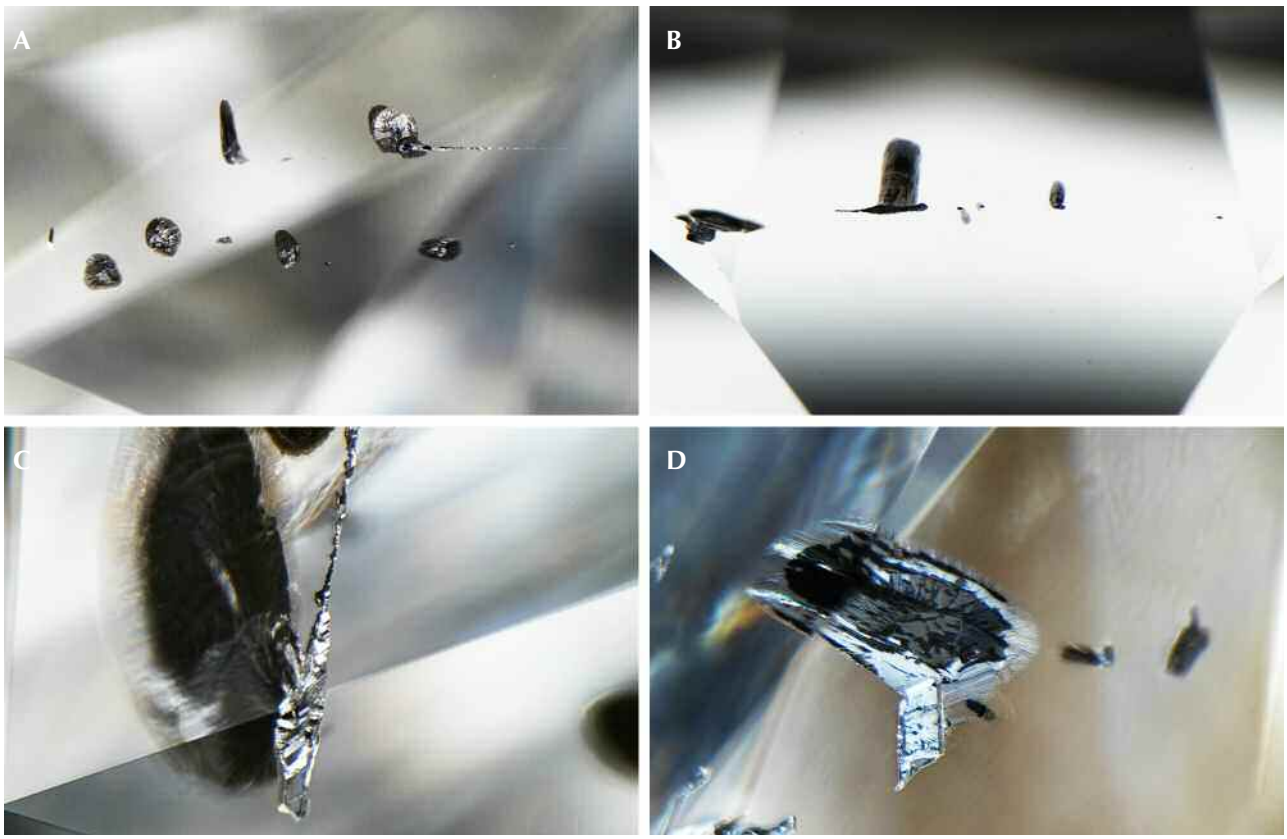

TABLE 1. Summary of inclusions observed in 83 CLIPPIR diamonds.

No. of diamonds	Largest in group	Inclusion assemblage	Inclusion properties	Mineralogy
60	30.13 ct	Metallic Fe-Ni-C-S (inferred to be primary melt inclusions)	Magnetic, silver/black color, opaque, grouped in <111> chains, CH_4 fluid jacket (22 also had detectable H_2 in Raman); associated with healed cracks; alters to red-brown (hematite).	Cohenite $(Fe,Ni)_3C$ + Fe-Ni alloy + pyrrhotite + minor phases
15	32.88 ct	Calcium silicate phases with original perovskite structure inferred (CaPv)	Colorless, transparent, often with droplet-like satellite inclusions defining lobes of localized healed cracks; one diamond had inclusions with CH_4 + H_2 fluid jackets but no indication of metal.	$CaSiO_3$-walstromite ± larnite (β-Ca_2SiO_4) ± $CaSi_2O_5$-titanite ± wollastonite ± perovskite ($CaTiO_3$)
4	10.21 ct	CaPv + metal	Colorless, transparent, with opaque, magnetic, metallic-luster droplet-like satellite inclusions with detectable CH_4; note that the silicate and metal co-occur rather than appearing as discrete separate inclusions.	$CaSiO_3$-walstromite ± larnite (β-Ca_2SiO_4) ± $CaSi_2O_5$-titanite + Fe-Ni-C-S phases
2	10.21 ct	Majoritic garnet + metal	Pale orange, transparent, with opaque, magnetic metallic phase partly occupying inclusion space, with detectable CH_4; note that the garnet and metal co-occur rather than appearing as discrete separate inclusions.	Low-Cr majoritic garnet ± Fe-Ni-C-S phases ± retrograde clinopyroxene, plagioclase, olivine
1	4.41 ct	CaPv + majoritic garnet + metal	Pale orange, transparent garnet inclusions with distinct metallic opaque regions exhibiting strong magnetism, with detectable CH_4; one colorless, transparent calcium silicate.	Majoritic garnet with metallic component + $CaSiO_3$-walstromite
1	10.17 ct	CaPv + majoritic garnet	Two colorless transparent calcium silicate inclusions; one pale orange, transparent garnet inclusion.	$CaSiO_3$-walstromite + majoritic garnet

Combines results from 53 diamonds in Smith et al. (2016) and 30 additional diamonds (see supplement at www.gia.edu/gems-gemology/winter-2017-worlds-biggest-diamonds). Average diamond mass is 6.1 ct, with 13 of them >10 ct. Note that most recorded masses are for the cut diamond and original mass of rough is unknown (also see data S1 in Smith et al., 2016).

The metallic inclusions (figures 3 and 5) have a silvery metallic luster with variable coating of patchy black graphite (as identified with Raman spectroscopy—a technique that can help identify minerals using a focused laser). They are bound by sharp-edged, flat cuboctahedral faces as well as complex stepped faces, and are often elongate in one dimension corresponding to a <111> vector with respect to the host diamond crystal. Inclusions near the surface of the diamond are noticeably magnetic when brought near a small rare-earth magnet suspended from a thread. Magnetism can be helpful for recognizing these inclusions but is not definitive since some other kinds of inclusions can be magnetic, such as sulfides or the metallic flux trapped in HPHT (high-pressure, high-temperature) synthetic diamonds. Raman spectroscopy, while of limited usefulness in identifying these inclusions since they are dominated by metals and carbides (both of which are inactive or weakly active in Raman), is good at revealing sulfides, which yield distinctive Raman peaks. We therefore take the general lack of Raman response from the inclusions with metallic luster as additional evidence that they are multi-phase metallic assemblages in which iron sulfide is a partial component rather than wholly sulfide mineral inclusions, which would have a distinctive Raman response.

Taken together, the metallic inclusions' consistent shape, texture, grouping, magnetism, lack of clear Raman response, and other features justify extending the microprobe and XRD results (Smith et al., 2016) to the majority of inclusions in the faceted samples that have been studied. It is unlikely that some of the metallic inclusions were misidentified sulfide inclusions. Furthermore, it is important to

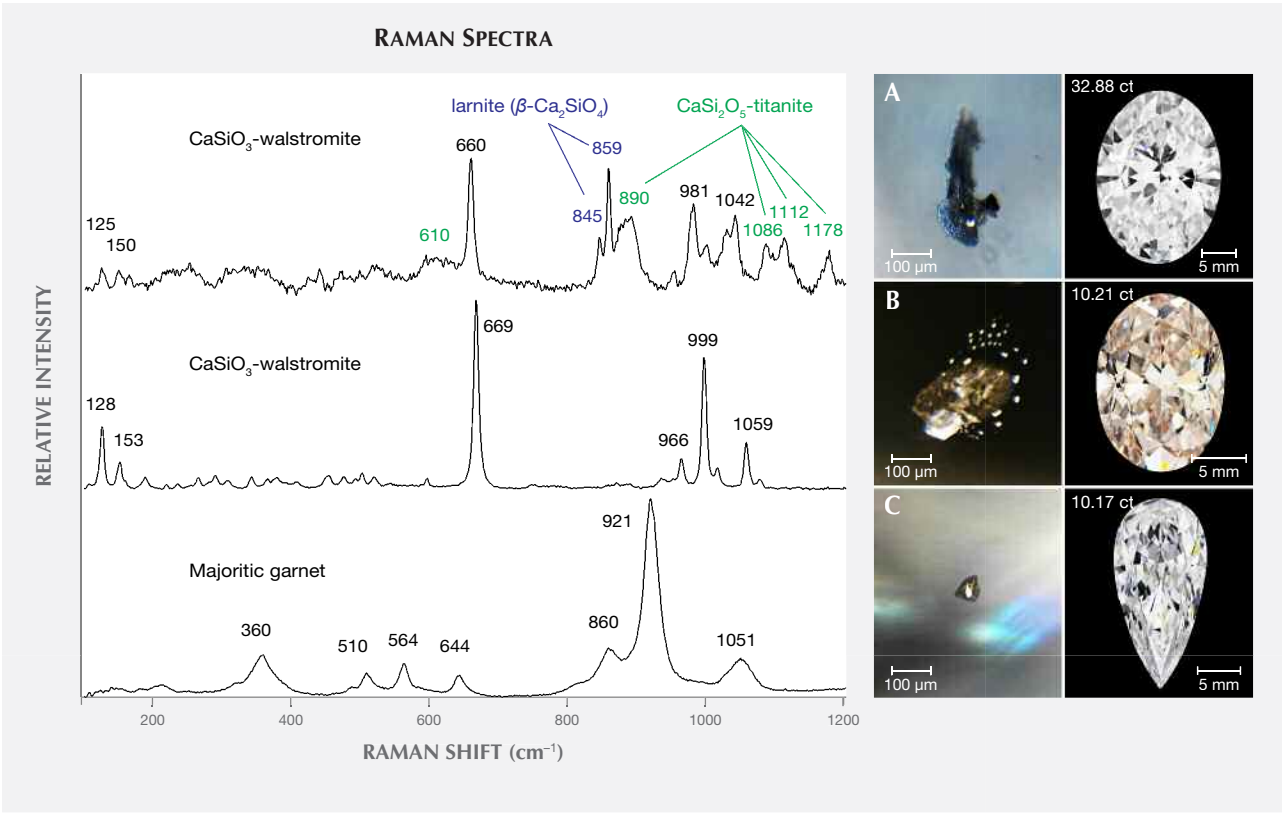

Figure 4. Raman spectra representative of the silicates in CLIPPIR diamonds. Spectra are offset vertically to avoid overlap. A: The principal silicate phase $CaSiO_3$-walstromite is accompanied by Ca_2SiO_4 and $CaSi_2O_5$ in a small colorless inclusion with a large graphitic fracture in a 32.88 ct D-color type IIa diamond. The middle spectrum shows $CaSiO_3$-walstromite alone, with peak positions noticeably shifted due to high remnant pressure inside the inclusion, on the order of several gigapascals (Anzolini et al., 2017). B: This $CaSiO_3$-walstromite inclusion in a 10.21 ct light pinkish brown type IIa diamond is a good example of the main part of the inclusion being accompanied by many smaller satellite inclusions, presumably from inclusion rupture/expansion during inversion from CaPv. C: Majoritic garnet in the bottom spectrum was observed in a 10.17 ct D-color type IIa diamond. Note this 10.17 ct sample contained both majorite and $CaSiO_3$-walstromite, and the bottom two spectra were actually both collected from this diamond. Photomicrographs by Evan M. Smith, face-up diamond photos by Jian Xin (Jae) Liao.

note that sulfide (pyrrhotite) appears to have been exsolved from the Fe-Ni-C-S mixture, suggesting that the original metallic liquid would have dissolved any sulfide minerals in this geologic environment, making it unlikely that discrete sulfide mineral grains would be available to be trapped as inclusions.

The fluid jacket with hydrogen and methane surrounding these inclusions is detectable with Raman spectroscopy, although the fluid is not uniformly distributed over the inclusion interface (figure 5). Methane (CH_4) is most easily detected and has a peak at 2918 cm^{-1}, while hydrogen (H_2) is generally less abundant but has its main peak at 4156 cm^{-1} (Smith et al., 2016). Peaks may be shifted by a few wavenumbers due to residual pressure inside the inclusions (Frezzotti et al., 2012). Methane is present at the inclusion-diamond interface in all metallic and most silicate inclusion assemblages in every CLIPPIR diamond and is often accompanied by hydrogen. The fluid is not thought to have existed as a free fluid phase while the diamond grew. Rather, it is interpreted to have formed as a result of hydrogen atoms exsolving out of the metallic liquid, and perhaps to some extent the silicates as well, forming CH_4 and H_2 by reacting with the surrounding diamond (Smith and Wang, 2016).

SILICATE INCLUSIONS IN CLIPPIR DIAMONDS: EVIDENCE FOR DEEP ORIGIN

The second most abundant inclusion is a mix of calcium silicates interpreted as retrogressed $CaSiO_3$-perovskite (CaPv), a perovskite-structured high-pressure mineral stable at depths beyond about 360 km (see box A and Brenker et al., 2005). The most common

BOX A: POST-ENTRAPMENT RECRYSTALLIZATION OF INCLUSIONS

Diamond excels at preserving trapped inclusions by virtue of its physical strength and chemical inertness. Even if they are protected and isolated, however, some inclusions may nevertheless recrystallize in response to the ambient temperature and pressure, especially when a diamond is transported to surface. This is true of the metallic Fe-Ni-C-S inclusions in CLIPPIR diamonds, which are thought to be trapped as a homogenous melt but later unmix into multiple phases (figure A-1). Textures within these metallic inclusions are essentially igneous, reflective of solidification and crystallization processes.

In addition to the crystallization of trapped melt inclusions, solid mineral phases can also undergo post-entrapment changes. Some minerals are only stable deep in the earth, at elevated pressure and temperature, and become unstable under conditions at the earth's surface. This is an important concept for inclusions in diamond because it explains how mineral inclusions can change after being trapped in a diamond. A mineral inclusion trapped very deep in the earth can undergo retrogression or inversion on its way to surface, meaning the inclusions we observe might be the breakdown products of some original high-pressure phase. When minerals break down, they are said to have undergone retrogression if the breakdown results in multiple phases, or inversion if the result is a single mineral phase. For example, the high-pressure mineral $CaSiO_3$-perovskite could undergo retrogression to produce two complementary minerals, larnite (β-Ca_2SiO_4) and $CaSi_2O_5$-titanite, or inversion to produce a single mineral, $CaSiO_3$-walstromite. In either case the bulk composition remains unchanged. Often, high-pressure phases are known mainly from experimental work and are referred to by their crystal structure. For example, the mineral perovskite ($CaTiO_3$) has a closely packed cubic crystal structure that is emulated by calcium silicate at high pressures, and this phase is called "perovskite" (broadly) or $CaSiO_3$-perovskite.

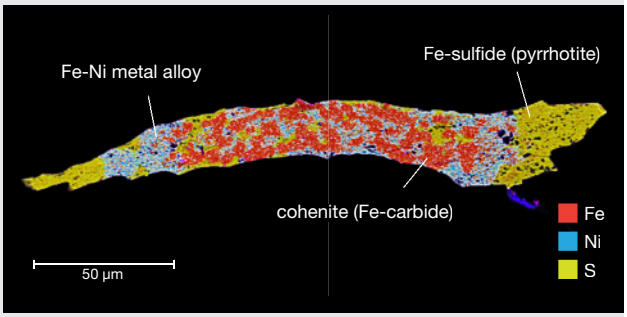

Figure A-1. An exposed polished metallic Fe-Ni-C-S inclusion. This inclusion was originally a homogeneous molten metal, but as it cooled and solidified the mixture crystallized into three separate phases: cohenite, Fe-Ni alloy, and Fe-sulfide. It is shown here as an energy-dispersive X-ray elemental map from an electron microscope, with the three phases colored according to where iron, nickel, and sulfur are more strongly concentrated. Fe (red) is concentrated in cohenite, Ni (blue) in Fe-Ni alloy, and S (yellow) in Fe-sulfide. The host diamond is a 2.14 ct offcut from a larger type IIa diamond from the Letšeng mine, Lesotho (sample Letseng_889, inclusion F). For methods, see Smith et al. (2016).

breakdown product of CaPv is $CaSiO_3$-walstromite (figure 4). Other calcium silicate phases encountered are larnite (β-Ca_2SiO_4), $CaSi_2O_5$-titanite, and, less commonly, wollastonite ($CaSiO_3$). All four phases are sometimes found together (metastably) in a single inclusion. If the inclusion contains sufficient titanium, it can be present as perovskite ($CaTiO_3$). Although it is still unclear, there may be two possible $CaSi_2O_5$ polymorphs in retrogressed high-pressure calcium silicate inclusions, corresponding to monoclinic and triclinic structures that have been observed in high-pressure experimental products (e.g., Kubo et al., 1997). Two different sets of Raman features have been interpreted as $CaSi_2O_5$-titanite. One signature encountered, as in figure 4, resembles monoclinic titanite ($CaTiSiO_5$) with its prominent 890 cm^{-1} band (see also database S3 in Smith et al., 2016). Another Raman signature corresponding to a synthetic $CaSi_2O_5$ sample (figure 2 in Nasdala et al., 2003) has also been observed in CaPv inclusions (Nasdala et al., 2003; Anzolini et al., 2016; Smith et al., 2016).

The CaPv inclusions are colorless and transparent, with surface textures ranging from flat-faced, sharp cuboctahedra to more ragged-looking irregular surfaces, especially for larger inclusions. Some inclusions have small opaque portions that are magnetic, interpreted as traces of metallic liquid trapped along with the silicate inclusion. Many CaPv inclusions possess small droplet-like satellite inclusions, all of the same mineralogy, grouped in one or more tabular lobes that appear to have been introduced from the main inclusion outward along localized cracks (figure 4B). The satellite inclusions are interpreted as the byproduct of pressure buildup sufficient to rupture

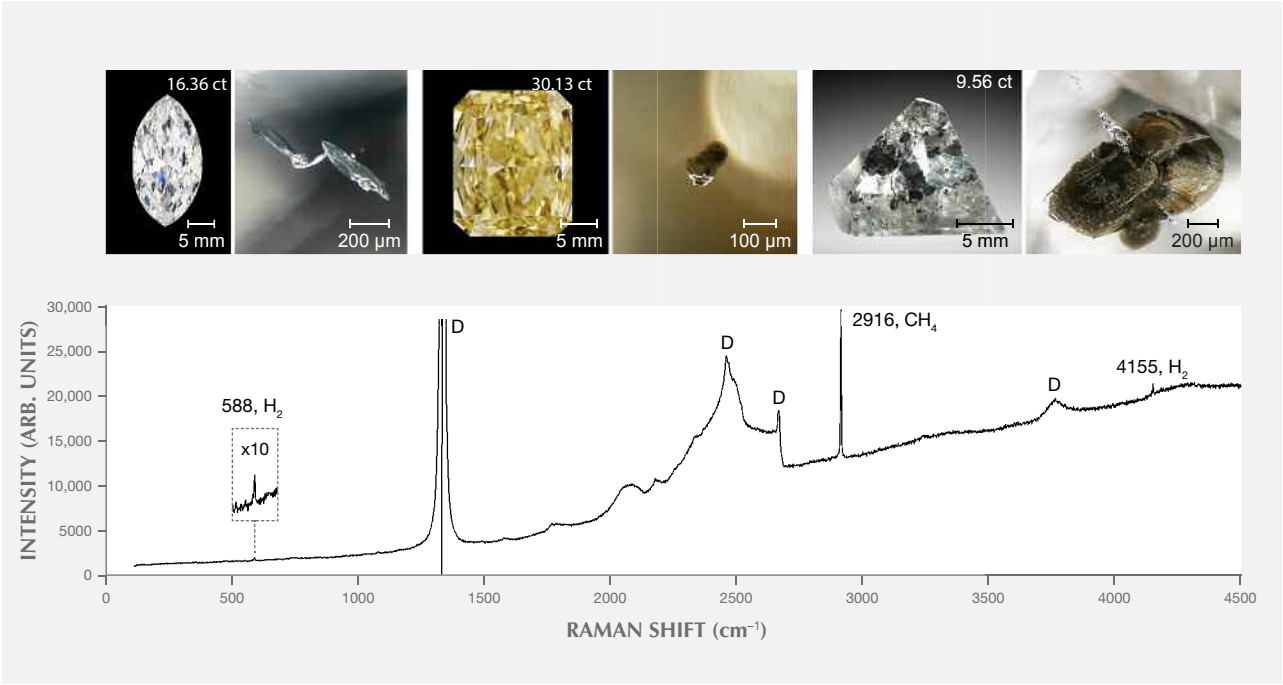

Figure 5. Metallic Fe-Ni-C-S inclusions with a representative Raman spectrum. All three CLIPPIR diamonds shown are type IIa. The faceted diamonds (left and center) are D-color and Fancy yellow-brown, respectively. The rightmost sample is a more heavily included offcut trimmed from an even larger, potentially D-color diamond. The Raman spectrum shows the typical lack of diagnostic mineral peaks (within the 100–1200 cm^{-1} range) coupled with methane (CH_4) and molecular hydrogen (H_2). Diamond Raman features are marked "D." Face-up faceted diamond photos (16.36 ct and 30.13 ct) by Jian Xin (Jae) Liao; other photos by Evan M. Smith.

the surrounding diamond, followed by injection of inclusion material out into the crack. A large volume increase of about 30% is estimated to accompany the inversion from CaPv to $CaSiO_3$-walstromite (Anzolini et al., 2016). The cracks have healed, and the diamond between individual satellite inclusions is optically continuous. Although this initial crack is healed, the main inclusion and sometimes even the satellite inclusions are each surrounded by a graphitic black fracture (figure 4B), an indication of further inclusion expansion during exhumation from the mantle by the erupting kimberlite. As a diamond is transported to the surface, the confining pressure acting on it gradually decreases and there is less pressure pushing in on its inclusions. In this situation, some inclusions push out against the diamond host, potentially causing a buildup of elastic strain and brittle rupturing around the inclusions. It is also possible that the surrounding diamond can deform plastically, thereby reducing the tendency for brittle failure. Such inclusions demonstrate the complex histories of brittle, elastic, and plastic deformation the host diamond can endure in response to inclusion pressure during ascent to surface.

An additional inclusion phase found was low-chrome majoritic garnet, a high-pressure form of garnet containing excess silica (figure 4C). The garnets are a pale orange color, again surrounded by large graphitic fractures, and sometimes have a coexisting magnetic, metallic component. The garnet provides a convenient maximum depth of derivation, since it is not stable deeper than about 750 km (Wijbrans et al., 2016). Silicate inclusion phases therefore bracket the depth between 360 and 750 km, overlapping the region of the mantle known as the mantle transition zone, which marks the transition between the upper mantle and lower mantle.

Examples of former $CaSiO_3$-perovskite (CaPv) and majoritic garnet inclusions coexisting with a metallic component and $CH_4 \pm H_2$ demonstrate a close association between the metal-only inclusions and the silicate-dominated inclusions and confirm that they are derived from a common, very oxygen-poor setting in the mantle. The best-studied example, since it

could be polished and examined in cross section with electron microscopy, is in one of the large diamond offcut samples from the Letšeng mine in Lesotho. In it, two majoritic garnets were observed, each trapped with a Fe-Ni-C-S metallic component alongside the garnet (fig S4 in Smith et al., 2016). The metallic accompaniments were a mixture of iron-carbide, Fe-Ni alloy, and Fe-sulfide, similar to the metallic inclusions seen in other diamonds containing no silicates. Again, CH_4 was present.

The silicate inclusions found in CLIPPIR diamonds are comparable to inclusions that have been described before in other sublithospheric diamonds (see summaries by Stachel et al., 2005; Kaminsky, 2012; Harte and Hudson, 2013). Here, these silicate inclusions are consistent with a mafic (eclogitic) host rock affiliation in the sublithospheric mantle. In the CLIPPIR diamond suite, however, the inclusion assemblages are somewhat different because they are associated with metal and the reduced volatiles methane and hydrogen.

CRYSTALLOGRAPHIC ORIENTATION OF METALLIC INCLUSIONS IN CLIPPIR DIAMONDS

In addition to their surprising metallic nature, the most common inclusions in CLIPPIR diamonds also have a spatial distribution that is striking. The metallic inclusions are often spatially grouped in one or more chains, all parallel to a single <111> vector (figure 6). This is a line oriented perpendicular to an octahedral {111} plane. Individual chains can waver slightly, with jogs and discontinuities, but can reach several millimeters in length. When multiple metallic inclusion chains are present, they are often parallel and define a pervasive linear fabric with no tendency to radiate from the center or otherwise align to any obvious diamond growth pattern. Instead the chains define a lineation within the diamond. The uniform, parallel, and crystallographically controlled orientation of the chains suggests they are like an overprinted fabric established after diamond growth. Cathodoluminescence or UV luminescence imaging sometimes reveals bright curviplanar features where the linear extension of an internal chain pierces the diamond surface. Figure 6 shows an example of these features extending radially from the point where an inclusion chain vector meets the polished surface. These otherwise invisible features are interpreted as healed cracks with roughly {110} orientation, of which there are three potential {110} plane orientations that intersect along the chain-defining <111>

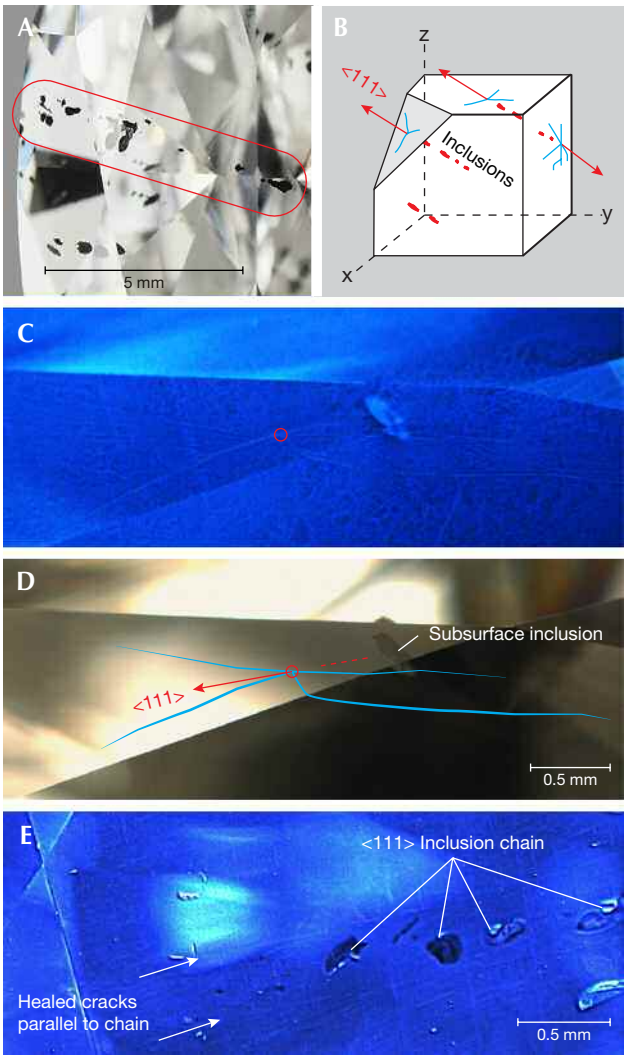

Figure 6. Metallic inclusions in CLIPPIR diamonds often occur in linear chains. A: Long, discontinuous inclusion chain in a 2.05 ct D-color type IIa diamond. B: Sketch showing a volume of diamond with multiple parallel <111> inclusion chains. Healed cracks of imperfect {110} orientation (blue) can be seen on the surface, at points where chain-defining vectors exit the diamond. C: DiamondView UV luminescence image revealing healed cracks related to a subsurface metallic inclusion in a 15.25 ct D-color type IIa diamond. Also visible are web-like dislocation networks. D: The same area shown in visible light, with blue traces drawn over the invisible healed cracks and the <111> vector extending from the inclusion, circled where the vector pierces the diamond surface. E: DiamondView image showing a <111> inclusion chain just below the surface, within the plane of the page, and two related healed cracks of {110} orientation running parallel to the inclusions. Two sets of finely spaced {111} slip traces are also seen, overprinting and cross-cutting the <111> vector and healed cracks. Photos by Evan M. Smith.

BOX B: DIAMOND DEFORMATION AS A WAY TO MAKE <111> CHAINS

Metallic inclusions in CLIPPIR diamonds frequently occur as chains of a few inclusions, aligned in a <111> crystallographic orientation (figures 3A, 3B, and 6). These chains are challenging to explain, but here we consider that they may be a consequence of diamond deformation in the mantle. At the elevated temperatures in the earth's mantle, diamond can deform plastically, though it can still develop cracks under high stress. If the 3-D stress is non-uniform and causes plastic deformation within the diamond, there will be a concentration of stress at the liquid metallic inclusions, where dislocation movement is interrupted and the inclusion itself is a strengthless fluid. Under these conditions, cracks might develop locally at the inclusion site. Given that the geometry of a <111> vector can be produced by the intersection of two or three {110} planes, the next step is to consider whether or not the diamond could crack on a {110} plane in a systematic way. In fact, brittle failure on {110} planes has been experimentally produced in diamond at elevated temperatures, concurrent with plastic deformation on {111} planes (Brookes et al., 1999). In this deformation experiment, the {110} cracks were parallel to the compressional axis.

Bulk plastic deformation of the diamond may have led to stress concentration and brittle failure localized at the metallic melt inclusions. The single <111> vector expressed by the chains could correspond to the direction of maximum compressive stress, resolved to the diamond lattice. At the inclusion site, {110} cracks can develop parallel to the compressional axis, like those observed by Brookes et al. in their deformation experiment. It would be possible to develop two or three symmetrically equivalent {110} cracks, such that the intersection of the cracks defines a short-lived dilatant <111> channel along which metallic melt inclusions can redistribute. In other words, the chains may be a redistribution of primary liquid metallic Fe-Ni-C-S inclusions, along a strain-controlled <111> direction, during brittle-plastic deformation of the diamond in the mantle. Redistribution of melt inclusions provides immediate local stress relief conducive to crack closure and healing. In two diamonds, the metallic inclusions have been observed as a planar group arranged in a {110} orientation, interpreted as a rare case of metallic liquid redistributed into a single planar {110} crack rather than the linear intersection of two or more cracks. Compared to the solid silicate inclusions, the metallic inclusions may be prone to this deformation-induced redistribution simply because they were in a liquid state. Inclusions containing both Fe-Ni-C-S metal and silicate trapped together do not exhibit the linear spatial distribution, possibly because the solid silicate portion strengthened the inclusion. It is very unlikely that the metallic liquid could have originated outside the diamond and penetrated into fine, parallel <111> channels. The graphitic {111} fractures currently visible around the Fe-Ni-C-S inclusions postdate this deformation.

The interpreted scenario of melt inclusion redistribution suggests these diamonds were deformed deep enough that the metallic inclusions were still liquid and had not unmixed. Development of the {110} healed cracks in the diamond likely predates the development of dislocation networks because dislocation networks appear to conform to the cracks rather than being crosscut by them. These two observations suggest that the development of <111> chains may have occurred in a discrete deformation episode at depth in the sublithospheric mantle. This deformation could be related to mantle convection and deep plate tectonic processes, or some other physical mechanism.

vector (see box B). The observations suggest that primary metallic melt inclusions were rearranged into chains during deformation of the host diamond at depth in the mantle. The significance is difficult to interpret without more detailed knowledge of the deformation behavior of diamond in the mantle, but likely speculation would relate diamond deformation to the pervasive deformation of mantle host rock that accompanies mantle convection.

METAL IN THE MANTLE: WHAT DOES IT MEAN?

Much of our knowledge of the earth comes from studying rocks near its surface, yet the deeper interior remains wholly inaccessible. While the continuous action of plate tectonics and the magmatism caused by it allows geologists to relate plate deformation and volcanism to Earth's deeper interior, magmas react, crystallize, and degas on their way to the surface, which changes their composition. The inevitably modified magmas make it difficult to discern the true nature of solid deeper mantle except by inference. It is well known that the increase in temperature and pressure with depth in the earth causes some minerals to break down and new minerals to form that are only stable at the more extreme pressure and temperature conditions. When considering the deep interior of the earth, this effect is fundamental. High-pressure experiments are used by scientists in the field of mineral

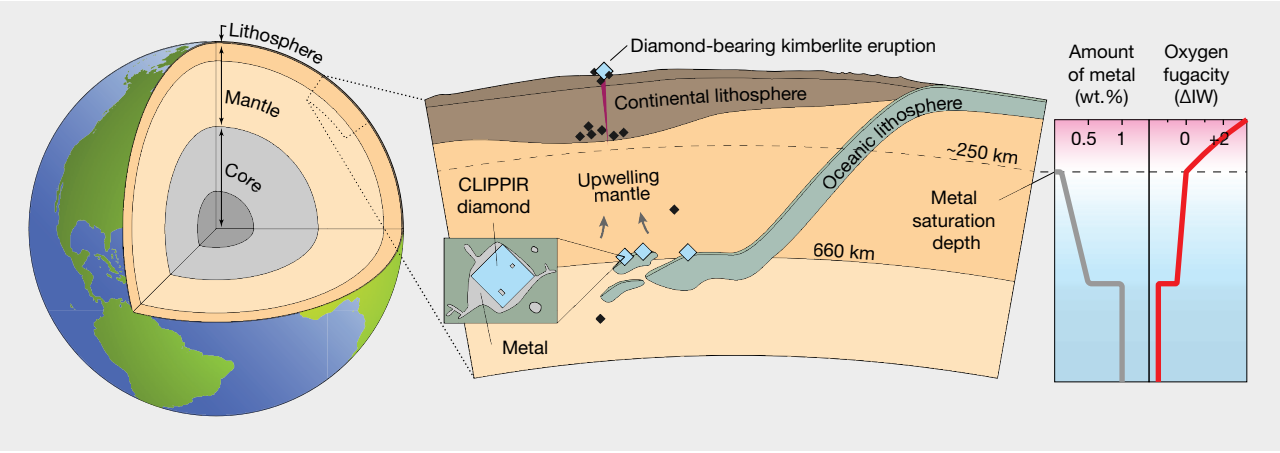

Figure 7. Cross section of the uppermost 1,000 km of the earth (center) illustrating the origin of CLIPPIR diamonds, shown as large blue diamond symbols. Smaller black diamond symbols indicate other varieties of diamond formed mainly in the continental lithosphere. Oceanic lithosphere subducted into the mantle provides the rocks necessary to explain the CaPv and majoritic garnet inclusions. CLIPPIR diamonds are thought to grow from liquid metal. Following growth, they may be carried upward with thermally or chemically buoyant upwelling mantle material and entrained in a kimberlite eruption to the surface. Profiles at the right show how the amount of metal in the mantle is expected to increase with depth starting from 250 km down, reaching up to approximately 1 wt.% below 660 km and buffering oxygen fugacity to reducing conditions (ΔIW, log units relative to the iron-wüstite buffer). Profiles after Rohrbach and Schmidt (2011).

physics to predict what kinds of mineral assemblages will occur even within the lower mantle. One important prediction to come out of these considerations of mineral physics is the idea that there is a depth, around 250 km, below which metallic iron might become one of the stable phases within deep mantle rocks (Frost et al., 2004). This prediction for metallic iron is fundamental to understanding the basic properties of the mantle. We know that at the bottom of the mantle it is in direct contact with the iron-nickel metal of the core, whereas at the top of the mantle, iron metal is not even stable during mantle melting. What happens, mineralogically speaking, in between?

The mechanism thought to be responsible is the progressive increase in the capacity for silicate minerals to host Fe^{3+} (iron with a 3+ oxidation state) relative to Fe^{2+} at high pressures (Ballhaus, 1995; Frost et al., 2004). The preference for Fe^{3+} in certain minerals under extreme pressure induces a disproportionation reaction, whereby valence electrons in the existing Fe^{2+} atoms are redistributed according to the reaction $3Fe^{2+} \rightarrow 2Fe^{3+} + Fe^{0}$. The Fe^{3+} is partitioned into the silicates, but the Fe^{0} separates into its own metallic phase. Iron disproportionation is thought to generate up to about 1 wt.% metal in the lower mantle (Frost et al., 2004; Rohrbach et al., 2007). Nickel, carbon, sulfur, and other elements are expected to dissolve into this metallic phase. This prediction is based on experiments (Bell et al., 1976; Ballhaus, 1995; Frost et al., 2004; Rohrbach et al., 2007; Rohrbach and Schmidt, 2011) but has never before been verified by actual observation of mineral grains.

The Fe-Ni-C-S melt inclusions in CLIPPIR diamonds are interpreted to be samples of such a metallic liquid, thereby confirming the fundamental process of Fe^{2+} disproportionation at depth (Smith et al., 2016) and providing evidence for a metallic liquid mechanism for diamond formation. This is the reason why CLIPPIR diamonds are so significant for earth science. The metal has large-scale implications for the behavior and evolution of the mantle over geologic time because it will influence the storage and cycling of the many elements that dissolve into it, such as oxygen, carbon, nitrogen, and hydrogen. The tendency for metallic iron to react with oxygen is expected to regulate or buffer the oxygen fugacity (the chemical availability of oxygen in the mantle) and maintain reducing conditions in the ambient mantle below about 250 km depth (figure 7). The projected low oxygen fugacity below 250 km, shown in figure 7, is a direct consequence of Fe^{2+} disproportionation (Rohrbach and Schmidt, 2011).

GEOLOGICAL ORIGIN OF CLIPPIR DIAMONDS

The consistent association of the mineral assemblages found in CLIPPIR diamonds with metal and methane, and its limitation to the CLIPPIR category, indicate that these diamonds form in a unique way. The CaPv and majoritic garnet inclusions, as well as the light carbon isotopes of the diamonds themselves, imply an association with subducted eclogite at extreme depths, likely within 360–750 km in the convecting mantle (Smith et al., 2016). This is much deeper than other gem diamonds, nearly all of which contain much more nitrogen (type I) and form in the lowermost parts of thick, old continental lithosphere at depths of 150–200 km. This extreme depth is, however, within the range of other rare "superdeep" diamonds in the sublithospheric mantle (figure 7).

The source of the carbon that crystallized into diamond is also important. Carbon has two stable isotopes, ^{13}C and ^{12}C, whose ratio varies according to the source, such as ambient mantle carbon or subducted, organic carbon. Variably light carbon isotopes in CLIPPIR diamonds, having $^{13}C/^{12}C$ ratios lower than the convecting mantle (Smith et al., 2016), suggest derivation from organic carbon (e.g., Kirkley et al., 1991; McCandless and Gurney, 1997), which implies the carbon was originally sourced at Earth's surface and then subducted.

CLIPPIR diamonds, as described above, appear to grow in close association with metallic liquid in the sublithospheric mantle. In this deep environment, the metallic Fe-Ni-C-S melt inclusions are hypothesized to represent small retained traces of the actual growth medium (Smith et al., 2016). Experiments and routine HPHT synthetic diamond growth processes show that iron-nickel mixtures are effective media at elevated temperatures and pressures, similar to the conditions in the deeper mantle. Diamond growth from metallic liquid could help explain the large size of CLIPPIR diamonds and their near-complete lack of nitrogen. Interestingly, the $CH_4 \pm H_2$ fluid jackets surrounding inclusions in natural CLIPPIR diamonds are a feature also seen in metal/carbide inclusions in HPHT synthetic diamonds (Smith and Wang, 2016), further supporting their interpretation as primary melt inclusions. Natural CLIPPIR diamonds may have crystallized inside small pockets of molten metallic liquid in Earth's deep mantle (figure 7). Small droplets of this metallic liquid would have occasionally been trapped within the diamonds as they grew, preserving the inclusion assemblages that we now sample.

As shown in figure 7, the eclogitic host rocks responsible for the silicate inclusions in CLIPPIR diamonds likely represent a basaltic crustal layer of the oceanic lithosphere that was subducted into the deeper underlying mantle. Below a depth of approximately 250 km, iron disproportionation can lead to metal saturation in mantle rocks. Both eclogite and the surrounding peridotite, including the mantle portion of the oceanic lithosphere, have the potential to generate metal by disproportionation. The source of the metal can be constrained by its bulk composition, roughly estimated as $Fe_{0.61–0.75}Ni_{0.10–0.13}C_{0.15–0.20}S_{0.05–0.12}$ based on the measured composition and relative cross-sectional area of cohenite, Fe-Ni alloy, and Fe-sulfide exposed in four polished inclusions (Smith et al., 2016). The modest Ni/(Ni+Fe) ratio (<0.2) is lower than the 0.3–0.5 range proposed for metal compositions precipitating in upper mantle peridotites (Rohrbach et al., 2014). Combined with the notion that the metallic liquid should be nearly immobile, tending to become trapped as disconnected droplets in the intergranular spaces of silicate mantle rocks (Rohrbach and Schmidt, 2011; Rohrbach et al., 2014), it is tempting to infer that the metal was generated locally, within the eclogitic host rocks where the diamonds grew. However, the observed Ni/S and Ni/(Ni+Fe) ratios in the inclusions are significantly higher than expected for equilibrium with eclogite (e.g., Ni/S=0.3 and Ni/(Ni+Fe)=0.02 reported for a metallic inclusion found in eclogitic garnet [Jacob et al., 2004]). To explain this discrepancy, the metal could have formed in equilibrium with peridotite (e.g., Zhang et al., 2016) and subsequently migrated into the eclogite before diamond crystallization occurred, but this scenario would imply significant metal precipitation, segregation, and liquid metal mobility in order for large diamonds to ultimately crystallize. If metal in the mantle is typically distributed along grain boundaries in silicates at low abundances of around 1%, then segregation and mobilization of the liquid metal may rely on deformation of surrounding rocks. However, other rock types or localized irregular rock compositions within the proposed growth setting of subducted oceanic lithosphere could also play a role in the metal and diamond formation. Further inclusion analyses and experimental constraints are needed to clarify the exact provenance of the metal.

Metallic iron has already been suggested to play a role in the formation of other types of superdeep diamonds, by its proposed ability to reduce subducted carbonate species (CO_3^{2-}) to diamond (C), also called "redox freezing" (Rohrbach and Schmidt, 2011). It is not clear how or even if carbonate would be involved

in CLIPPIR diamond growth since an oxygen-deficient mantle region is a prerequisite for metallic inclusions. But the expected high calcium content of carbonate might be one explanation for the abundance of CaPv inclusions as a reaction byproduct (Walter et al., 2008; Bulanova et al., 2010; Harte and Richardson, 2012; Thomson et al., 2016). Alternatively, other forms of subducted carbon such as abiogenic, organic carbon could be involved where carbonate does not play a significant role. The main point here is that metallic Fe-Ni-C-S inclusions clearly show that the metallic iron-rich phase plays the key role for CLIPPIR superdeep diamond formation.

Once formed, CLIPPIR diamonds, like other sublithospheric diamonds, require some mechanism to transport them upward to be sampled by kimberlite magmatism and brought to surface where they are mined. The mechanism is uncertain but may involve thermochemically buoyant, ascending solid mantle that is part of the general upwelling associated with mantle convection (figure 7) prior to being entrained in erupting kimberlite. The dynamic action of the mantle may be cryptically recorded in the crystal strain in CLIPPIR diamonds. There is a remarkably strong association between CLIPPIR diamonds and dislocation networks (De Corte et al., 2006) that can be better understood in light of the present study. This web-like feature, rare in other diamonds, is visible in cathodoluminescence or UV fluorescence imaging in almost all 83 CLIPPIR samples examined (e.g., figure 6C). The network is interpreted as a dislocation structure arising from plastic deformation followed by recovery (Hanley et al., 1977). The high temperatures afforded by a sublithospheric origin as well as the minimal nitrogen contents in CLIPPIR diamonds are conducive to the development of dislocation networks. These diamonds have witnessed severe conditions in the deep mantle—a likely consequence of mantle convection. Earth's mantle convects in the solid form, introducing strain on the scale of the mineral lattice at extremely high pressure. Despite their often exquisite gem quality, these diamonds have an internal structure that preserves evidence of this strain and their journey from the deep mantle to the surface.

CONCLUSIONS

It has long been recognized that a curiously high proportion of large, gem-quality diamonds are type IIa, an otherwise rare designation. But now we have learned that these special gems, termed CLIPPIR diamonds, actually form in a unique way, in a different part of the mantle compared to other kinds of diamonds. Many inclusion-free, nitrogen-deficient diamonds, especially those with dislocation networks, are expected to belong to the CLIPPIR category (figure 2). The "superdeep" (i.e., sublithospheric) origin of CLIPPIR diamonds, which leaves them free of inclusions associated with shallower, lithospheric mantle diamond host rocks, helps explain why exploration geologists and miners have never been able to correlate these diamonds with traditional indicator minerals (Bowen et al., 2009; Gurney and Helmstaedt, 2012). The rarity and extraordinary value that have made research study prohibitive over the years also contributes to this fact. Indicator minerals such as chrome-rich pyrope and ilmenite, the fragments of diamond host rocks from the lithospheric mantle keels of Archean continents, are useful for finding lithospheric diamonds. CLIPPIR diamonds, however, originate deeper in the mantle, far below the lithosphere where these indicator minerals are not stable and cannot be included. Finding CLIPPIR diamonds is all the more difficult. Predicting their ore grade, even in promising mines, requires large bulk sampling and carries great uncertainty.

Large and pure diamonds are nevertheless a highly sought prize. Prior to the study by Smith et al. (2016), there was no accepted model describing how these large type IIa diamonds form in nature. We can now appreciate that these exceptional diamonds are coincidentally some of the most scientifically valuable samples of our planet's interior. They are a window into the deep convecting mantle, providing a glimpse through the shroud of Earth's tectonic plates and surface magmatism.

Previous experiments and theory have predicted for many years that parts of the deep mantle below about 250 km contain small amounts of metallic iron and have limited available oxygen. Now, the metallic inclusions and their surrounding methane and hydrogen jackets in CLIPPIR diamonds provide physical evidence to support this prediction. This is a key observation for our understanding of planet Earth, having broad implications for its geologic evolution through time, such as the behavior and cycling of carbon and hydrogen, which are the primary fluxes for rock melting and the generation of new crust. Confirming the existence of metallic iron containing nickel, carbon, sulfur, and other elements as a discrete liquid also impacts our understanding of the seismic velocity and thermal and electrical conductivity of the mantle, as well as the way it deforms and flows. This result is a sign that there is still much to be learned from diamonds and their inclusions.

ABOUT THE AUTHORS

Dr. Smith is a research scientist, and Dr. Wang is vice president of research and development, at GIA in New York. Dr. Shirey is a senior scientist in the Department of Terrestrial Magnetism of the Carnegie Institution for Science in Washington, DC.

ACKNOWLEDGMENTS

The authors thank GIA's Ulrika D'Haenens-Johansson and Paul Johnson for assistance with sample selection, Alex Balter for help handling data for figure 2, and Jian Xin (Jae) Liao for acquiring face-up images of the diamonds in figures 4 and 5. This work was completed with the support of GIA's Liddicoat Postdoctoral Research Fellowship program.

REFERENCES

Anzolini C., Angel R., Merlini M., Derzsi M., Tokár K., Milani S., Krebs M., Brenker F., Nestola F., Harris J. (2016) Depth of formation of $CaSiO_3$-walstromite included in super-deep diamonds. *Lithos*, Vol. 265, pp. 138–147, http://dx.doi.org/10.1016/j.lithos.2016.09.025

Anzolini C., Prencipe M., Alvaro M., Romano C., Vona A., Lorenzon S., Smith E.M., Brenker F.E., Nestola F. (2017) Depth of formation of super-deep diamonds: Raman barometry of $CaSiO_3$-walstromite inclusions. *American Mineralogist*, in press.

Ballhaus C. (1995) Is the upper mantle metal-saturated? *Earth and Planetary Science Letters*, Vol. 132, No. 1-4, pp. 75–86, http://dx.doi.org/10.1016/0012-821X(95)00047-G

Bell P., Mao H., Weeks R., Valkenburg A. (1976) High pressure disproportionation study of iron in synthetic basalt glass. *Carnegie Institution of Washington Yearbook 1975*, pp. 515–520.

Bowen D.C., Ferraris R.D., Palmer C.E., Ward J.D. (2009) On the unusual characteristics of the diamonds from Letšeng-la-Terae kimberlites, Lesotho. *Lithos*, Vol. 112S, pp. 767–774, http://dx.doi.org/10.1016/j.lithos.2009.04.026

Breeding C.M., Shigley J.E. (2009) The "type" classification system of diamonds and its importance in gemology. *G&G*, Vol. 45, No. 2, pp. 96–111, http://dx.doi.org/10.5741/GEMS.45.2.96

Brenker F.E., Vincze L., Vekemans B., Nasdala L., Stachel T., Vollmer C., Kersten M., Somogyi A., Adams F., Joswig W. (2005) Detection of a Ca-rich lithology in the Earth's deep (> 300 km) convecting mantle. *Earth and Planetary Science Letters*, Vol. 236, No. 3-4, pp. 579–587, http://dx.doi.org/10.1016/j.epsl.2005.05.021

Brookes E., Greenwood P., Xing G. (1999) The plastic deformation and strain-induced fracture of natural and synthetic diamond. *Diamond and Related Materials*, Vol. 8, No. 8-9, pp. 1536–1539, http://dx.doi.org/10.1016/S0925-9635(99)00080-1

Bulanova G.P., Walter M.J., Smith C.B., Kohn S.C., Armstrong L.S., Blundy J., Gobbo L. (2010) Mineral inclusions in sublithospheric diamonds from Collier 4 kimberlite pipe, Juina, Brazil: Subducted protoliths, carbonated melts and primary kimberlite magmatism. *Contributions to Mineralogy and Petrology,* Vol. 160, No. 4, pp. 489–510, http://dx.doi.org/10.1007/s00410-010-0490-6

Crookes W. (1909) *Diamonds*. Harper & Brothers, London, New York.

De Corte K., Anthonis A., Van Royen J., Blanchaert M., Barjon J., Willems B. (2006) Overview of dislocation networks in natural type IIa diamonds. *G&G*, Vol. 42, No. 3, pp. 122–123.

Frezzotti M.L., Tecce F., Casagli A. (2012) Raman spectroscopy for fluid inclusion analysis. *Journal of Geochemical Exploration*, Vol. 112, pp. 1–20, http://dx.doi.org/10.1016/j.gexplo.2011.09.009

Frost D.J., Liebske C., Langenhorst F., McCammon C.A., Trønnes R.G., Rubie D.C. (2004) Experimental evidence for the existence of iron-rich metal in the Earth's lower mantle. *Nature*, Vol. 428, No. 6981, pp. 409–412, http://dx.doi.org/10.1038/nature02413

Gurney J.J., Helmstaedt H.H. (2012) The origins of type IIa diamonds and their enhanced economic significance. *10th International Kimberlite Conference, Short Abstract No. 10IKC-123*, pp. 247–248.

Gurney J.J., Helmstaedt H.H., Richardson S.H., Shirey S.B. (2010) Diamonds through time. *Economic Geology*, Vol. 105, No. 3, pp. 689–712, http://dx.doi.org/10.2113/gsecongeo.105.3.689

Hanley P.L., Kiflawi I., Lang A.R. (1977) On topographically identifiable sources of cathodoluminescence in natural diamonds. *Philosophical Transactions of the Royal Society of London. Series A, Mathematical and Physical Sciences*, Vol. 284, No. 1324, pp. 329–368, http://dx.doi.org/10.1098/rsta.1977.0012

Harte B., Hudson N.C.F. (2013) Mineral associations in diamonds from the lowermost upper mantle and uppermost lower mantle. *Proceedings of 10th International Kimberlite Conference: Volume 1*, pp. 235–253.

Harte B., Richardson S. (2012) Mineral inclusions in diamonds track the evolution of a Mesozoic subducted slab beneath West Gondwanaland. *Gondwana Research*, Vol. 21, No. 1, pp. 236–245, http://dx.doi.org/10.1016/j.gr.2011.07.001

Iron in diamonds (1877) *Scientific American Supplement*, Vol. 3, p. 877.

Jacob D.E., Kronz A., Viljoen K.S. (2004) Cohenite, native iron and troilite inclusions in garnets from polycrystalline diamond aggregates. *Contributions to Mineralogy and Petrology,* Vol. 146, No. 5, pp. 566–576, http://dx.doi.org/10.1007/s00410-003-0518-2

Kaminsky F. (2012) Mineralogy of the lower mantle: A review of 'super-deep' mineral inclusions in diamond. *Earth-Science Reviews*, Vol. 110, No. 1-4. pp. 127–147, http://dx.doi.org/10.1016/j.earscirev.2011.10.005

Kaminsky F.V., Wirth R. (2011) Iron carbide inclusions in lower-mantle diamond from Juina, Brazil. *Canadian Mineralogist*, Vol. 49, No. 2, pp. 555–572, http://dx.doi.org/10.3749/canmin.49.2.555

Kirkley M.B., Gurney J.J., Otter M.L., Hill S.J., Daniels L.R. (1991) The application of C isotope measurements to the identification of the sources of C in diamonds: a review. *Applied Geochemistry*, Vol. 6, No. 5, pp. 477–494, http://dx.doi.org/10.1016/0883-2927(91)90048-T

Kubo A., Suzuki T., Akaogi M. (1997) High pressure phase equilibria in the system $CaTiO_3$-$CaSiO_3$: stability of perovskite solid solutions. *Physics and Chemistry of Minerals*, Vol. 24, No. 7, pp. 488–494, http://dx.doi.org/10.1007/s002690050063

McCandless T.E., Gurney J.J. (1997) Diamond eclogites: comparison with carbonaceous chondrites, carbonaceous shales, and microbial carbon-enriched MORB. *Russian Geology and Geophysics*, Vol. 38, No. 2, pp. 394–404.

Mikhail S., Guillermier C., Franchi I.A., Beard A.D., Crispin K., Verchovsky A.B., Jones A.P., Milledge H.J. (2014) Empirical evidence for the fractionation of carbon isotopes between diamond and iron carbide from the Earth's mantle. *Geochemistry,*

Geophysics, Geosystems, Vol. 15, No. 4, pp. 855–866, http://dx.doi.org/10.1002/2013GC005138
Moore A.E. (2014) The origin of large irregular gem-quality type II diamonds and the rarity of blue type IIb varieties. *South African Journal of Geology*, Vol. 117, No. 2, pp. 219–236, http://dx.doi.org/10.2113/gssajg.117.2.219
Nasdala L., Brenker F.E., Glinnemann J., Hofmeister W., Gasparik T., Harris J.W., Stachel T., Reese I. (2003) Spectroscopic 2D-tomography: Residual pressure and strain around mineral inclusions in diamonds. *European Journal of Mineralogy*, Vol. 15, No. 6, pp. 931–935, http://dx.doi.org/10.1127/0935-1221/2003/0015-0931
Rohrbach A., Schmidt M.W. (2011) Redox freezing and melting in the Earth's deep mantle resulting from carbon-iron redox coupling. *Nature*, Vol. 472, No. 7342, pp. 209–212, http://dx.doi.org/10.1038/nature09899
Rohrbach A., Ballhaus C., Golla-Schindler U., Ulmer P., Kamenetsky V.S., Kuzmin D.V. (2007) Metal saturation in the upper mantle. *Nature*, Vol. 449, No. 7161, pp. 456–458, http://dx.doi.org/10.1038/nature06183
Rohrbach A., Ghosh S., Schmidt M.W., Wijbrans C.H., Klemme S. (2014) The stability of Fe–Ni carbides in the Earth's mantle: Evidence for a low Fe–Ni–C melt fraction in the deep mantle. *Earth and Planetary Science Letters*, Vol. 388, pp. 211–221, http://dx.doi.org/10.1016/j.epsl.2013.12.007
Scarratt K., Shor R. (2006) The Cullinan diamond centennial: A history and gemological analysis of Cullinans I and II. *G&G*, Vol. 42, No. 2, pp. 120–132, http://dx.doi.org/10.5741/GEMS.42.2.120
Sharp W.E. (1966) Pyrrhotite: A common inclusion in South African diamonds. *Nature*, Vol. 211, No. 5047, pp. 402–403, http://dx.doi.org/10.1038/211402b0
Shirey S.B., Shigley J.E. (2013) Recent advances in understanding the geology of diamonds. *G&G*, Vol. 49, No. 4, pp. 188–222, http://dx.doi.org/10.5741/GEMS.49.4.188
Smith E.M., Wang W. (2016) Fluid CH_4 and H_2 trapped around metallic inclusions in HPHT synthetic diamond. *Diamond and Related Materials*, Vol. 68, pp. 10–12, http://dx.doi.org/10.1016/j.diamond.2016.05.010
Smith E.M., Shirey S.B., Nestola F., Bullock E.S., Wang J., Richardson S.H., Wang W. (2016) Large gem diamonds from metallic liquid in Earth's deep mantle. *Science*, Vol. 354, No. 6318, pp. 1403–1405, http://dx.doi.org/10.1126/science.aal1303
Stachel T., Harris J.W. (2009) Formation of diamond in the Earth's mantle. *Journal of Physics: Condensed Matter*, Vol. 21, No. 36, 364206, http://dx.doi.org/10.1088/0953-8984/21/36/364206
Stachel T., Brey G., Harris J.W. (2005) Inclusions in sublithospheric diamonds: glimpses of deep earth. *Elements*, Vol. 1, No. 2, pp. 73–78, http://dx.doi.org/10.2113/gselements.1.2.73
Thomson A.R., Walter M.J., Kohn S.C., Brooker R.A. (2016) Slab melting as a barrier to deep carbon subduction. *Nature*, Vol. 529, No. 7584, pp. 76–79, http://dx.doi.org/10.1038/nature16174
Walter M.J., Bulanova G.P., Armstrong L.S., Keshav S., Blundy J.D., Gudfinnsson G., Lord O.T., Lennie A.R., Clark S.M., Smith C.B., Gobbo L. (2008) Primary carbonatite melt from deeply subducted oceanic crust. *Nature*, Vol. 454, No. 7204, pp. 622–625, http://dx.doi.org/10.1038/nature07132
Wijbrans C.H., Rohrbach A., Klemme S. (2016) An experimental investigation of the stability of majoritic garnet in the Earth's mantle and an improved majorite geobarometer. *Contributions to Mineralogy and Petrology*, Vol. 171, No. 5, pp. 1–20, http://dx.doi.org/10.1007/s00410-016-1255-7
Wilks J., Wilks E. (1994) *Properties and Applications of Diamond*. Butterworth-Heinemann, Oxford, UK.
Zhang Z., Dorfman S.M., Labidi J., Zhang S., Li M., Manga M., Stixrude L., McDonough W.F., Williams Q. (2016) Primordial metallic melt in the deep mantle. *Geophysical Research Letters*, Vol. 43, No. 8, pp. 3693–3699, http://dx.doi.org/10.1002/2016GL068560